Carbohydrate Polymers 117 (2015) 408–413

Contents lists available at ScienceDirect

Carbohydrate Polymers

journal homepage: www.elsevier.com/locate/carbpol

Facile fabrication of hierarchical cellulose nanospicules via hydrolytic hydrogenation

Kesavan Devarayan[b], Hak-Yong Kim[a,b], Byoung-Suhk Kim[a,b,*]

[a] Department of Organic Materials & Fiber Engineering, Chonbuk National University, 567 Baekje-daero, Deokjin-gu, Jeonju-si 561-756, Jeollabuk-do, Republic of Korea
[b] Department of BIN Fusion Technology, Chonbuk National University, 567 Baekje-daero, Deokjin-gu, Jeonju-si 561-756, Jeollabuk-do, Republic of Korea

ARTICLE INFO

Article history:
Received 4 September 2014
Received in revised form
22 September 2014
Accepted 3 October 2014
Available online 12 October 2014

Keywords:
Cellulose nanospicules
Hydrolytic hydrogenation
Hierarchical nanostructures
Electrospinning
Cellulose nanorods

ABSTRACT

A new spicule-like cellulose nanostructure is prepared from electrospun cellulose nanofibers using a one-pot bifunctional catalysis strategy namely hydrolytic hydrogenation. The electrospun cellulose nanofibers or cellulose film was treated in presence of catalyst consisting of an alkali and a metal to produce celluloses with structures like nanospicules, nanoflowers or nanorods, respectively. This work highlights the promising combination of electrospinning and hydrolysis/hydrogenation for facile production of hierarchical cellulose nanostructures such as nanospicules and nanorods.

1. Introduction

Polymers from renewable natural resources are very useful raw materials in day-to-day life. Among natural polymers, cellulose is the most abundant polysaccharide that constitutes approximately 1.5×10^{12} t of total biomass produced in a year (Klemm, Schmauder, & Heinze, 2002). The major sources are wood and plant, whereas tunicates, bacteria and algae are also known to produce cellulose (Moon, Martini, Nairn, Simonsen, & Youngblood, 2011). Traditionally, cellulose is used for two general purposes. On one hand, it has been used as a raw material for manufacturing of commodities such as paper, board, and textile fibers. On the other hand, it is utilized as a precursor to produce artificial cellulose-based threads and films by means of chemical conversions. The major attraction for research on cellulose is not only because of abundance and economy but also due to its unique structure combined with properties such as biocompatibility, hydrophilicity, and the presence of reactive hydroxyl groups, which allows introduction of new functionalities that are useful for several applications (Heinze & Liebert, 2001).

Nanofabrication technology is a potential tool to modify the properties of natural polymers for sustainable developments (Na et al., 2014; Yinjuan et al., 2013). In view of green chemistry principles, the interests in nanomaterials have shifted toward the use of cellulose in recent years. Cellulose itself is not ascertained as a highly performing material, while hierarchical nanostructures that compose of cellulose fibers opens up opportunities for a wide range of applications in technical textiles, medical industries, and separation techniques. Based on the morphology, nanocellulose is classified into three types namely (i) cellulose nanofibers, (ii) cellulose micro/nanofibrils, and (iii) cellulose micro/nanocrystals or cellulose nanowhiskers (Moon et al., 2011; TAPPI, 2012). Different methods have been developed in recent decades to produce these nanocellulosic materials by adopting mainly two principles, broadly known as physical and chemical modifications. In physical methods, the cellulose is subjected to mechanical processes such as ultrasonication (Johnson, Zink-Sharp, Renneckar, & Glasser, 2009; Wang & Cheng, 2009), high-pressure homogenization (Stelte & Sanadi, 2009; Turbak, Snyder, & Sandberg, 1983), grinding/crushing (Iwamoto, Nakagaito, & Yano, 2007; Chakraborty, Sain, & Kortschot, 2005), and/or microfluidization to produce micro/nanofibrillated cellulose. In the case of chemical method, the micro/nanocrystalline cellulose is produced by an acid hydrolysis treatment. Both techniques involve in pre-treatment, mostly TEMPO oxidation (Saito, Nishiyama, Putaux, Vignon, & Isogai, 2006),

* Corresponding author at: Department of Organic Materials and Fiber Engineering, Chonbuk National University, 567 Baekje-daero, Deokjin-gu, Jeonju 561-756, Republic of Korea. Tel.: +82 632702352; fax: +82 632702348.
E-mail addresses: kbsuhk@jbnu.ac.kr, kbsuhk@yahoo.com (B.-S. Kim).

http://dx.doi.org/10.1016/j.carbpol.2014.10.002
0144-8617/

followed by disintegration, deconstruction or depolymerization of the cellulose. Electrospinning is also the other versatile technique for production of electrospun non-woven mats of cellulose nanofibers (Cs-ESNWs) (Greiner & Wendorff, 2007).

Inspired by the hydrogen formation in alkaline corrosion reactions of aluminium, in this study, a novel strategy combining electrospinning and hydrolytic hydrogenation is used to produce unique cellulose nanospicules. To the best of our knowledge, for the first time, herein we introduce a new type of nanocellulose consisting of spicule-like nanostructures obtained by in situ hydrolysis/hydrogenation technique. Hydrolytic hydrogenation has become a widespread technique until recently after successful catalytic conversion of polysaccharides into low molecular weight saccharides. Hydrolytic hydrogenation is a bifunctional catalytic strategy consisting of a transition metal catalyst and a dilute acid or an acidic solid support (Vyver, Geboers, Jacobs, & Sels, 2011). For the first time, we demonstrate hydrolytic hydrogenation of cellulose using weak alkaline solution. By effectively controlling the hydrolysis/hydrogenation of electrospun cellulose nanofiber mats and films, new cellulose nanostructures were produced in this study.

2. Experimental

2.1. Electrospinning

The solution of cellulose acetate (CA, M_n = 50,000 g/mol, Aldrich) was prepared using dimethylacetamide/acetone (volume ratio = 1:2) at the concentration of 7–8 wt%. The solution was placed in a 10-mL syringe attached to a plastic tip with an inner diameter of 0.6 mm. The electrospinning was carried out at 9.5 kV (NanoNC power supply, Republic of Korea) at a tip-to-collector distance of 18 cm at about 25 °C and relative humidity of 45–50%. The electrospun fibers were collected on a grounded aluminium foil followed by drying at 25 °C in vacuum for 24 h and then stored at room temperature until further use (Khatri, Wei, Kim, & Kim, 2012; Kim & Kim, 2011).

2.2. Preparation of cellulose nanostructures

At first, the CA electrospun non-woven (CA-ESNW) mat collected on an aluminium foil was cut into small pieces (ca. 4 × 5 cm). Secondly, a set of CA-ESNW mats were peeled-off and deacetylated in 0.05 M NaOH solution for 24 h at 25 °C to regenerate cellulose nanofibers (*P-Cs-ESNWs*) (Liu & Hsieh, 2002). Another set of CA-ESNW mats with aluminium foil were treated in 20 mL of aqueous alkaline solutions having 0.05 M, 0.1 M, 0.5 M, and 1.0 M of NaOH at ambient conditions. After a specific treatment time (1.5 min, 3 min, and 5 min), the aluminium foil was removed from the alkaline solution and further continued the treatment of CA-ESNW in alkaline solution for another 24 h under mechanical shaking in order to obtain regenerated cellulose fibers. Then the cellulose nanofiber mats were washed with distilled water for at least 3 times at the interval of 5 h followed by drying in vacuum for 24 h at 25 °C to obtain *H-Cs-ESNWs*. On the other hand, CA films were cast on aluminium foil using 7 wt% of CA solution followed by drying in vacuum for 24 h at 25 °C. The films were treated in alkaline solutions similar to the CA nanofiber mats. The mean thickness of the resulting cellulose fibers and film were measured as 70 and 10 μm, respectively, using a digital micrometer (Mitutoyo ABSOLUTE) with a resolution of 1 μm.

2.3. Characterization

Scanning electron microscopy (SEM) images were taken using a JEOL JSM-5900 scanning electron microscope after sputtering the samples with platinum for 120 s. Energy dispersive X-ray measurements were conducted using the EDAX system attached to the same microscope. A field-emission microscope (FE-SEM) was also used to observe the morphologies after sputtering the samples with osmium for 7 s. X-ray diffraction (XRD) patterns were recorded on a Rikaku X-ray diffractometer (Cu $K\alpha$ radiation).

A CA-ESNW mat was hydrolysis/hydrogenated in 1.0 M NaOH. After 10 min the nanofiber mat was completely solubilized in 1.0 M NaOH. Then the solution was neutralized using 1.0 M HCl and the fragments were analyzed by Fourier-transform infrared spectroscopy (FT-IR, Perkin Elmer) and liquid chromatography–mass spectrometry (LC/MS spectrometer, Agilent 1100 LC/MS).

3. Results and discussion

Two sets of experiments were carried out for the preparation of hierarchical cellulose nanostructures. In the first experiment, the alkali treatment of cellulose acetate (CA) nanofibers that were electrospun on aluminium foil was investigated. On one hand, the CA-ESNW nanofiber mats were peeled-off (P) from the aluminium foil and deacetylated in 0.05 M NaOH solution (Fig. 1a) to regenerate the cellulose-nanofibers (Cs-ESNW). These regenerated cellulose nanofiber mats were indicated by *P-Cs-ESNW*. On the other hand, the CA nanofibers on aluminium foil were directly treated in aqueous NaOH solutions of varying concentrations (0.05–1.0 M NaOH) for a relatively short time ranging from 1.5 to 3 min. These samples were indicated by *H-Cs-ESNWs*. Fig. 1b–d shows the morphological changes in regenerated cellulose fibers upon treatment with alkaline solution. With very low concentration of NaOH and short treatment time, for instance, 0.05 M NaOH and 3.0 min, the cellulose fibers developed a spicule-like nanostructure. Fig. 1d shows the magnified FE-SEM image of cellulose nanofibers with spicule-like nanostructures. It clearly reveals that parts of the cellulose nanofibers split into spicules that still stuck on the originating fiber surface. Furthermore, X-ray diffraction (XRD) patterns of *H-Cs-ESNW* and *P-Cs-ESNWs* exhibited peaks at $2\theta = 20.3^\circ$ and 22.7° corresponding to (4.31 Å) and (3.94 Å) d-spacing, which are characteristics of cellulose I structure (Fig. 2) (Nishiyama, Langan, & Chanzy, 2002; Teixeira et al., 2010). The XRD results revealed that the ordered structure of the crystalline region on the *H-Cs-ESNW* is not disrupted by hydrolysis/hydrogenation. In other words, spicule-like crystalline nanostructures can be produced via a simple hydrolysis/hydrogenation technique.

At about 3.0 min of alkaline treatment in 0.05 M NaOH, the fiber mats get detached from the aluminium foil due to rapid evolution of hydrogen gas. Meanwhile, increase in the alkaline strength from 0.05 to 0.1 and 0.5 M NaOH indicated the development of a non-homogeneous flower-like nanostructure in the cellulose fibers (Fig. 3a). Further increase in the concentration of alkali has led to the dissolution of cellulose fibers as seen in Fig. 3b. For the ease of understanding, the splitting up of cellulose nanofibers into spicule-like nanostructure can be compared to the blossoming of a bud to a flower, where one edge of the petal are attached to the stem of the flower.

The anomalous behavior of cellulose fibers in presence of aluminium and NaOH can be explained by means of hydrolysis/hydrogenation mechanism. Aluminium is readily corroded in alkaline environment even at room temperature. The combination of aluminium/aqueous NaOH is a well-known system for hydrogen production (Belitskus, 1970; Soler, Candela, Macanás, Muñoz, & Casado, 2009; Martíneza, Benítesa, Gallegosa, & Sebastiàn, 2005) and is represented by the following series of reactions.

$$2Al + 6H_2O + 2NaOH \rightarrow 2NaAl(OH)_4 + 3H_2 \quad (1)$$

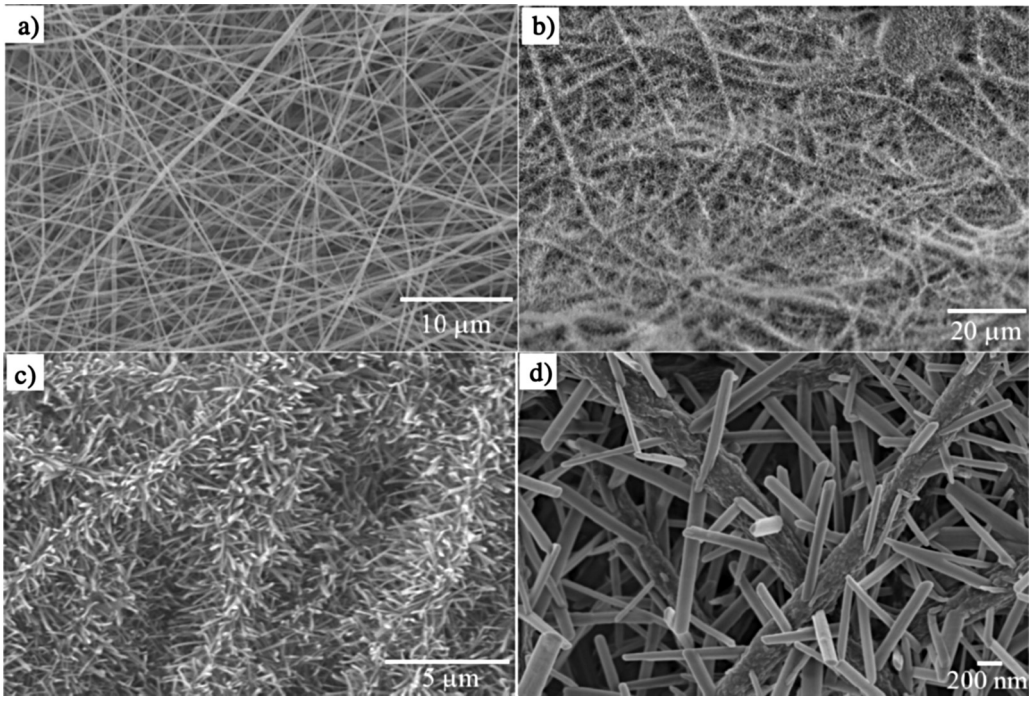

Fig. 1. SEM images of regenerated cellulose nanofibers (a) and development of hierarchical nanospicules in *H-Cs-ESNW* nanofibers after treatment in 0.05 M NaOH for 3 min (b and c) and FE-SEM image (d) of hierarchical nanospicules in cellulose nanofibers.

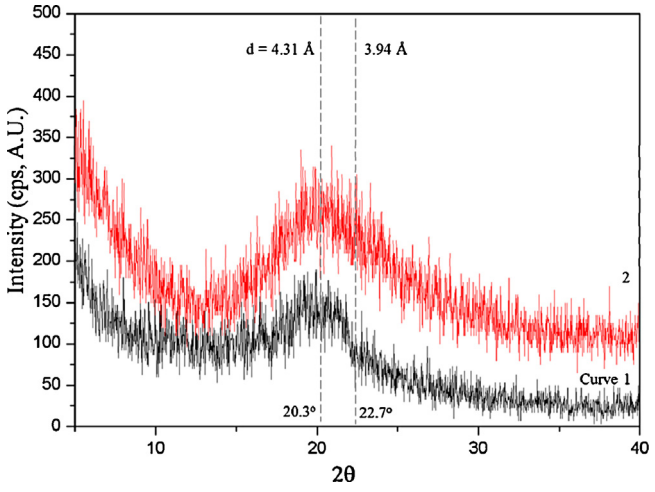

Fig. 2. XRD patterns of *P-Cs-ESNW* mat (Curve 1) and *H-Cs-ESNW* mat (Curve 2). Peaks at $2\theta = 20.3^{\circ}$ and 22.7° corresponding to (4.31 Å) and (3.94 Å) d-spacing, which are characteristics of cellulose I structure.

$$NaAl(OH)_4 \rightarrow NaOH + Al(OH)_3 \quad (2)$$

$$2Al + 6H_2O \rightarrow 2Al(OH)_3 + 3H_2 \quad (3)$$

In Eq. (1), it is shown that the sodium hydroxide is consumed to produce hydrogen gas. But when the concentration of sodium aluminate ($NaAl(OH)_4$) exceeds the saturation limit, sodium aluminate decomposes to regenerate sodium hydroxide along with aluminium hydroxide (Eq. (2); Belitskus, 1970). The overall reaction of hydrogen production is represented by Eq. (3). Generally, aluminium is well protected by a dense oxide layer formed on its surface due to their strong affinity for oxygen. However, alkaline solutions are strong enough to destroy the protective oxide layer to produce hydrogen gas. Accordingly, in this study, hydrogen evolution was not observed until 1.5 min in 0.05 M NaOH solution (Wang, Leung, Leung, & Ni, 2009). It is proposed that the elemental hydrogen evolved from the corrosion reactions of aluminium foil with aqueous NaOH solutions causes the hydrolysis/hydrogenation of the glycoside bonds in the cellulose backbone leading to deconstruction of cellulose nanofibers into spicule-like nanostructures. In order to support this mechanism, a cellulose nanofiber mat was subjected to hydrolysis/hydrogenation for 10 min in 1.0 M

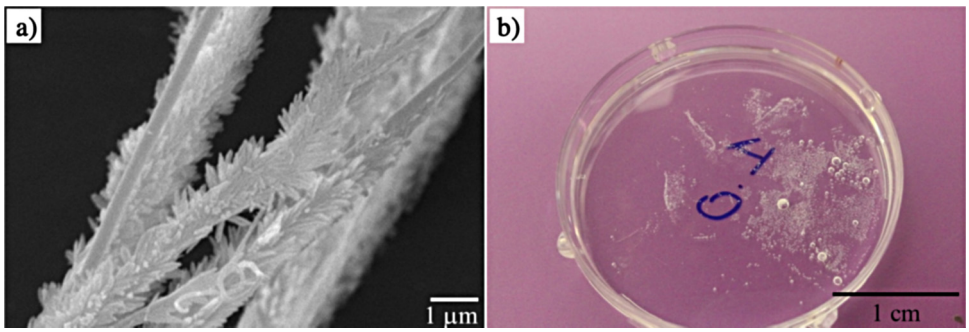

Fig. 3. Effect of NaOH concentration on development of non-homogeneous flower-like cellulose nanostructures on treatment of cellulose fibers with (a) 0.1 M NaOH and (b) dissolution of cellulose nanofibers in 1.0 M NaOH after hydrolytic hydrogenation.

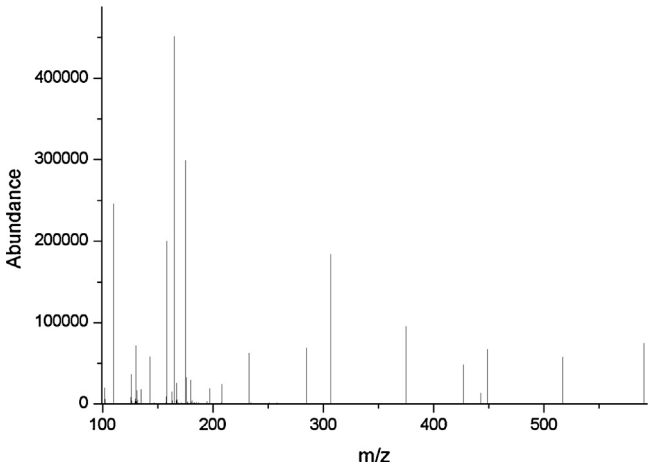

Fig. 4. ES-MS results extracted from LC–MS data of hydrolytic hydrogenated CA-ESNW nanofibers in 1.0 M NaOH for 10 min. The fragments corresponding to *m*/*z* values were assigned to low molecular weight saccharides as given in Table 1.

Table 1
The ESI-mass spectral data for the products obtained upon hydrogenation of CA-ESNW nanofibers in 1.0 M NaOH for 10 min.

m/*z*, Molecular species	Molecular formula	Assigned compound	RA%
110.0, $[M]^+$	$C_6H_6O_2$	MF	54.4
126.0, $[M]^+$	$C_6H_6O_3$	HF	11.2
158.0, $[M]^+$	$C_6H_6O_5$	DF	44.3
164.9, $[M+H]^+$	$C_6H_{12}O_5$	DG	100.0
180.2, $[M]^+$	$C_6H_{12}O_6$	Glc	1.5
306.8, $[M-H]^+$	$C_{12}H_{19}O_9$	AP-DG	60.8
442.7, $[M]^+$	$C_{17}H_{30}O_{13}$	Xyl-DG	3.0
448.8, $[M-H]^+$	$C_{18}H_{25}O_{13}$	HF-Glc_2	14.9
474.4, $[M]^+$	$C_{17}H_{30}O_{15}$	Glc_2-Xyl	1.8
658.8, $[M+Na]^+$	$C_{23}H_{40}O_{20}$	Glc_3-Xyl	7.4

Where, MF—methylfural; HF—5-hydroxymethylfurfual DF—3,4-dihydroxy-5-acetyl-2-furanone; VAP—1,6-anhydro-D-glucopyranose; DG—2-deoxy-D-glucose; Xyl—xylose; Glc—glucose; RA%—relative abundance percentage.

NaOH, which is sufficient condition for complete dissolution and analysed by liquid chromatography–mass spectrometry (LC–MS). The mass spectral results revealed that the identified fragments were of low molecular weight saccharides such as D-glucose and other hydrolysis products of cellulose (Fig. 4 and Table 1). The LC–MS results confirmed the dissolution of cellulose nanofibers by hydrolysis/hydrogenation in 1.0 M NaOH (Fig. 3b), which indicated that prolonged hydrolysis/hydrogenation treatment of cellulose nanofibers leads to depolymerization of cellulose molecules.

The FT-IR spectrum of hydrolysis/hydrogenated CA-ESNW exhibited characteristic peaks corresponding to predominant fragments such as glucose and furfural derivatives as shown in Fig. 5 (Curve 2). Generally, the carbohydrates show characteristic peaks of C—O and C—C in the region of 1550 to 600 cm^{-1}. A broad peak observed in the region of 3600 to 2900 cm^{-1} was assigned to both O—H and C—H stretching vibrations. A combination of O—C—H and C—O—H were observed from 1660 to 1471 cm^{-1}. The in plane deformation of C—H and O—H were exhibited between 1450 to 1341 cm^{-1}. The C—H and O—H deformation were observed from 1230 to 1037 cm^{-1}. The shart peak at 994 cm^{-1} is assigned to stretching and bending vibrations of C—H. It should be noted that no peak for C=O streatching vibration corresponding to cellulose acetate was observed for the hydrolytically hydrogenated sample (Fig. 5). It is proposed that the Al/NaOH system may play an efficient role of depolymerization of the cellulose via non-stereospecific hydrolytic hydrogenation as well as deacetylation. Accordingly, hierarchical cellulose nanostructures can be produced by hydrolysis/hydrogenation technique by tuning time scale and alkaline concentrations.

The elemental compositions found by SEM–EDS also supported the claim by FT-IR results (data not shown). That is, the weight%s of carbon and oxygen present in the CA-ESNW mats treated in 1.0 M NaOH for 10 min were closely match with the values of the regenerated cellulose nanofiber mats, suggesting that both depolymerization and deacetylation occurs simulataneously.

As a comparison to the Cs-ESNW nanofiber mats, the next set of experiments was performed on the effect of alkaline treatment on the cellulose acetate film cast on aluminium foil. Similar to the CA-ESNW mats, alkaline treatments were given to CA films to obtain regenerated cellulose films. Fig. 6a–d shows the SEM morphologies of cellulose films treated with different concentrations of NaOH. Treatment of CA films in 0.05, 0.1, and 0.5 M NaOH for upto 2 min did not yield any microscopically observable hierarchical nanostructures as seen in Fig. 5a. While increasing the concentration of NaOH to 1.0 M, short nanorods or whisker-like nanostructures were observed (Fig. 6b–d). Fig. 5b shows that these

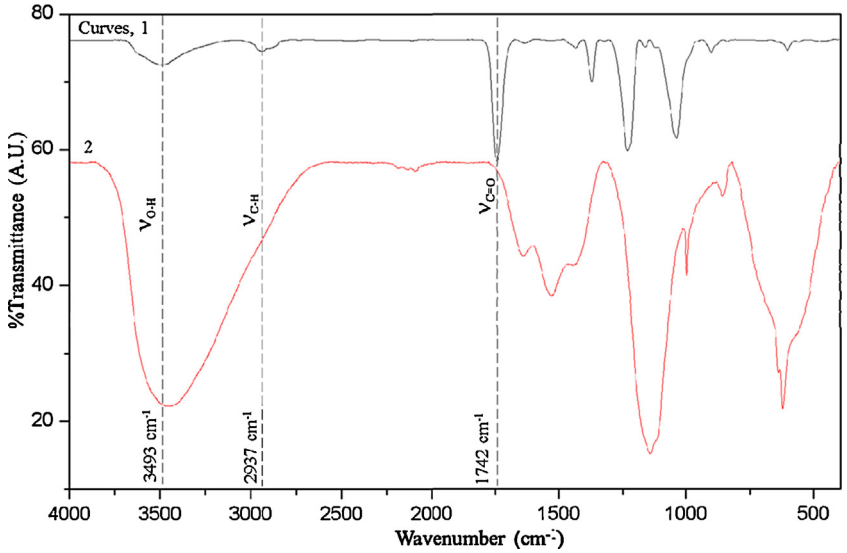

Fig. 5. ATR-FTIR spectra of as spun CA-ESNW (Curve 1), and CA-ESNW treated in 1.0 M NaOH for 10 min (Curve 2). Disappearance of C=O stretching vibration of acetyl groups of CA in Curve 2 suggests that hydrolytic hydrogenation in presence of Al foil is non-stereoselective in nature.

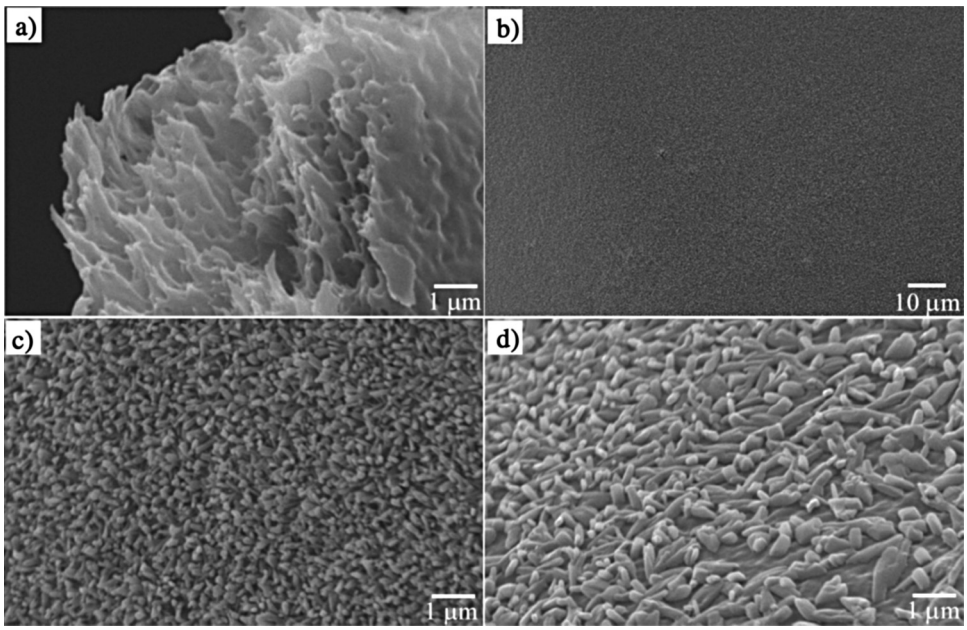

Fig. 6. Effect of NaOH concentration on cellulose film treated in (a) 0.05 M NaOH and (b) 1.0 M NaOH for 2 min via hydrolysis/hydrogenation. The figures (c) and (d) are magnified image of (b), which is close view of the nanostructures on hydrolysis/hydrogenated cellulose film.

nanostructures are produced homogeneously on the surface of the regenerated cellulose film. Magnified SEM images at 30° tilt (Fig. 6c and d) provides a better view on close packing of the nanostructures on regenerated cellulose film. The above results indicated that by controlling the strength of alkaline medium and time scale via hydrolysis/hydrogenation, hierarchical nanostructures can be produced from cellulose films.

4. Conclusion

The present study showed that the combination of electrospinning and hydrolysis/hydrogenation is a simple and inexpensive technique involving in a mild one-pot procedure for preparation of hierarchical nanostructures, such as nanospicules from nanofibers and nanorods from films, which can be amendable to the large scale preparation of various composite structures of polysaccharides. In most cases, hydrolysis/hydrogenation of cellulose is carried out either in hydrogen atmosphere or by means of transfer hydrogenation by selecting suitable solvent in acidic environment (Vyver et al., 2011). The major advantages of this Al/NaOH catalytic system is that it is not only useful to produce nanospicules from nanofibers and nanorods from films, but also advantageous for producing low molecular weight saccharides via depolymerization, which gives insight for production of energy, biofuel, and other useful chemicals from renewable biomass (Kobayashi, Matsuhashi, Komanoya, Hara, & Fukuoka, 2011). A good balance of catalytic functions, for instance, the time and NaOH concentration, is the most important to produce the unique spicule-like and rod-like nanocelluloses.

Acknowledgements

This work was supported by the Basic Science Research Program through the National Research Foundation of Korea (NRF) funded by the Ministry of Education (1301001076) and financially supported by the Brain Korea 21 PLUS Project, NRF. This work was also supported by the Basic Research Laboratory Program (2014R1A4A1008140) through the Ministry of Science, ICT & Future Planning and by the National Research Foundation of Korea (NRF) grant funded by the Korean Government (MSIP) (no. 2014R1A4A1008140) and by the "Robot industrial cluster construction program" through the Ministry of Trade, Industry & Energy (MOTIE).

References

Belitskus, D. (1970). Reaction of aluminum with sodium hydroxide solution as a source of hydrogen. *Journal of Electrochemical Society*, *117*, 1097–1099.
Chakraborty, A., Sain, M., & Kortschot, M. (2005). Cellulose microfibrils: A novel method of preparation using high shear refining and cryocrushing. *Holzforschung*, *59*, 102–107.
Greiner, A., & Wendorff, J. H. (2007). Electrospinning: A fascinating method for the preparation of ultrathin fibers. *Angewandte Chemie International Edition*, *46*, 5670–5703.
Heinze, T., & Liebert, T. (2001). Unconventional methods in cellulose functionalization. *Progress in Polymer Science*, *26*, 1689–1762.
Iwamoto, S., Nakagaito, A. N., & Yano, H. (2007). Nano-fibrillation of pulp fibers for the processing of transparent nanocomposites. *Applied Physics A*, *89*, 461–466.
Johnson, R. K., Zink-Sharp, A., Renneckar, S. H., & Glasser, W. G. (2009). A new bio-based nanocomposite: Fibrillated TEMPO-oxidized celluloses in hydroxypropylcellulose matrix. *Cellulose*, *16*, 227–238.
Khatri, Z., Wei, K., Kim, B-S., & Kim, I-S. (2012). Effect of deacetylation on wicking behavior of co-electrospun cellulose acetate/polyvinyl alcohol nanofibers blend. *Carbohydrate Polymers*, *87*, 2183–2188.
Kim, B-S., & Kim, I-S. (2011). Recent nanofiber technologies. *Polymer Reviews*, *51*, 235–238.
Klemm P D, Schmauder, H-P., & Heinze, T. (2002). Polysaccharides II: Polysaccharides from Eukaryotes. In E. Vandamme, S. D. Beats, & A. Steinbüchel (Eds.), *Biopolymers* (vol. 2) (p. 290). Weinheim: Wiley-VCH.
Kobayashi, H., Matsuhashi, H., Komanoya, T., Hara, K., & Fukuoka, A. (2011). Transfer hydrogenation of cellulose to sugar alcohols over supported ruthenium catalysts. *Chemical Communications*, *47*, 2366–2368.
Liu, H., & Hsieh, Y-L. (2002). Ultrafine fibrous cellulose membranes from electrospinning of cellulose acetate. *Journal of Polymer Science, B: Polymer Physics*, *40*, 2119–2129.
Moon, R. J., Martini, A., Nairn, J., Simonsen, J., & Youngblood, J. (2011). Cellulose nanomaterials review: Structure, properties and nanocomposites. *Chemical Society Review*, *40*, 3941–3994.
Na, W., Xianfeng, W., Yongtang, J., Xiaoqi, L., Jianyong, Y., & Bin, D. (2014). Electrospun nanofibrous chitosan membranes modified with polyethyleneimine for formaldehyde detection. *Carbohydrate Polymers*, *108*, 192–199.
Nishiyama, Y., Langan, P., & Chanzy, H. (2002). Crystal structure and hydrogen-bonding system in cellulose I beta from synchrotron X-ray and neutron fiber diffraction. *Journal of American Chemical Society*, *124*, 9074–9082.
Martíneza, S. S., Benítesa, W. L., Gallegosa, A. A. Á., & Sebastiàn, P. J. (2005). Recycling of aluminum to produce green energy. *Solar Energy Materials & Solar Cells*, *88*, 237–243.
Saito, T., Nishiyama, Y., Putaux, J-L., Vignon, M., & Isogai, A. (2006). Homogeneous suspensions of individualized microfibrils from TEMPO-catalyzed oxidation of native cellulose. *Biomacromolecules*, *7*, 1687–1691.
Soler, L., Candela, A. M., Macanás, J., Muûoz, M., & Casado, J. (2009). In situ generation of hydrogen from water by aluminum corrosion in solutions of sodium aluminate. *Journal of Power Sources*, *192*, 21–26.

Stelte, W., & Sanadi, A. R. (2009). Preparation and characterization of cellulose nanofibers from two commercial hardwood and softwood pulps. *Industrial & Engineering Chemistry Research*, *48*, 11211–11219.

TAPPI WI 3021. (2012). *Standard terms and their definition for cellulose nanomaterial*. TAPPI.

Teixeira, E. d-M., Corrêa, A. C., Manzoli, A., Leite, F. d-L., Oliveira, C. R-d., & Mattoso, L. H. C. (2010). Cellulose nanofibers from white and naturally coloredcotton fibers. *Cellulose*, *17*, 595–606.

Turbak, A., Snyder, F., & Sandberg, K. (1983). Microfibrillated cellulose: A new cellulose product: Properties, uses, and commercial potential. *Journal of Applied Polymer Science Polymer Symposium*, *37*, 815–827.

Vyver, S. V-d, Geboers, J., Jacobs, P. A., & Sels, B. F. (2011). Recent advances in the catalytic conversion of cellulose. *ChemCatChem*, *3*, 82–94.

Wang, S., & Cheng, Q. (2009). A novel process to isolate fibrils from cellulose fibers by high-intensity ultrasonication, Part 1: Process optimization. *Journal of Applied Polymer Science*, *113*, 1270–1275.

Wang, H. Z., Leung, D. Y. C., Leung, M. K. H., & Ni, M. (2009). A review on hydrogen production using aluminum and aluminum alloys. *Renewable and Sustainable Energy Reviews*, *13*, 845–853.

Yinjuan, H., Shenglong, D., Mingzhu, L., Chunmei, G., Jinlong, Y., Xinjie, Z., et al. (2013). Ultra-small and anionic starch nanospheres: Formation and vitro thrombolytic behavior study. *Carbohydrate Polymers*, *96*, 426–434.